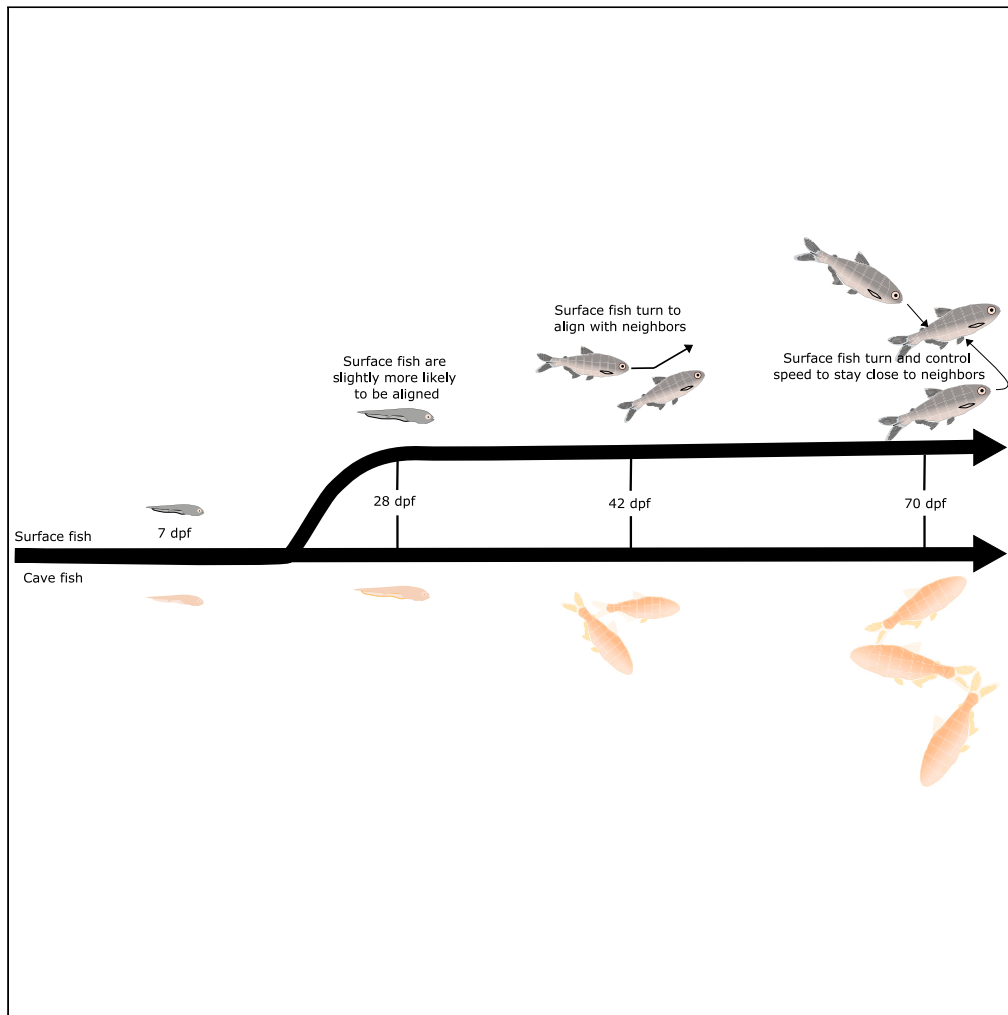


Article

Changes in local interaction rules during ontogeny underlie the evolution of collective behavior



Alexandra Paz,
Karla J. Holt, Anik
Clarke, ..., Erik R.
Duboué, Yaouen
Fily, Johanna E.
Kowalko

yfily@fau.edu (Y.F.)
jok421@lehigh.edu (J.E.K.)

Highlights
Schooling behavior
emerges over the course
of development in
Astyanax surface fish

Tendency to align
develops prior to
attraction in surface fish

Cavefish do not show the
transition to alignment or
attraction found in surface
fish

Reduced turning and
speeding relative to
neighbors contributes to
loss of schooling

Paz et al., iScience 26, 107431
September 15, 2023 © 2023
The Authors.
<https://doi.org/10.1016/j.isci.2023.107431>

Article

Changes in local interaction rules during ontogeny underlie the evolution of collective behavior

Alexandra Paz,¹ Karla J. Holt,¹ Anik Clarke,¹ Ari Aviles,¹ Briana Abraham,¹ Alex C. Keene,² Erik R. Duboué,¹ Yaouen Fily,^{1,*} and Johanna E. Kowalko^{3,4,*}

SUMMARY

Collective motion emerges from individual interactions which produce group-wide patterns in behavior. While adaptive changes to collective motion are observed across animal species, how local interactions change when these collective behaviors evolve is poorly understood. Here, we use the Mexican tetra, *Astyanax mexicanus*, which exists as a schooling surface form and a non-schooling cave form, to study differences in how fish alter their swimming in response to neighbors across ontogeny and between evolutionarily diverged populations. We find that surface fish undergo a transition to schooling mediated by changes in the way fish modulate speed and turning relative to neighbors. This transition begins with the tendency to align to neighbors emerging by 28 days post-fertilization and ends with the emergence of robust attraction by 70 days post-fertilization. Cavefish exhibit neither alignment nor attraction at any stage of development. These results reveal how evolution alters local interactions to produce striking differences in collective behavior.

INTRODUCTION

Social behaviors in animals are critical for survival, and extensive variation in sociality is found across animal species. Collective motion, which includes flocking in birds, herd migration in ungulates, and swarming in insects, is an example of collective behavior in which individuals' responses to local social cues culminate in coordinated behavioral outcomes.^{1–8} Collective motion is also observed in many species of fish, and includes shoaling and schooling.^{9–14} Shoaling is defined as fish maintaining close proximities to other individuals in the group, while schooling is characterized by fish maintaining both close proximity and alignment. While shoaling and schooling result in complex collective motion in groups of up to thousands of individuals, these group dynamics emerge from local interactions between individuals within the group, such as individuals moving toward or away from neighbors based on their relative position.^{11,15–17} How these local interactions manifest in group level dynamics has been established in various fish species that display robust schooling and shoaling.^{11,15,18–23} However, how evolution impacts these local interaction rules to produce group level differences in collective behaviors is poorly understood. Establishing how changes to individual behaviors lead to variation in collective motion is critical to revealing how collective behaviors evolve in natural populations.

The Mexican tetra, *Astyanax mexicanus*, is a species of freshwater fish that consists of surface populations which inhabit rivers and streams in Mexico and Southern Texas, and multiple independently evolved cave fish populations that inhabit caves in Northeastern Mexico.^{24–27} Caves inhabited by *A. mexicanus* have a number of differences in ecology relative to the surface habitat, including constant darkness, loss of macroscopic predators, and differences in water chemistry.^{27–33} These ecological differences have resulted in the repeated evolution of a number of morphological, physiological, and behavioral traits in *A. mexicanus* cave fish relative to their surface conspecifics, including loss or reduction of eyes and pigmentation, enhancement of non-visual sensory systems, changes to metabolism, and reductions in sleep.^{26,34–43} *A. mexicanus* cave fish have also evolved changes to multiple social behaviors relative to surface fish, including reduced aggression and an absence of social hierarchies.^{44–48} Further, while adult surface fish exhibit robust shoaling and schooling in the lab and in the field, these behaviors are reduced in adult fish from multiple cave fish populations.^{49–53} Thus, the robust differences in schooling and shoaling

¹Wilkes Honors College, Florida Atlantic University, Jupiter, FL 33458, USA

²Department of Biology, Texas A&M, College Station, TX 77840, USA

³Department of Biological Sciences, Lehigh University, Bethlehem, PA 18015, USA

⁴Lead contact

*Correspondence:
yfily@fau.edu (Y.F.),
jok421@lehigh.edu (J.E.K.)
<https://doi.org/10.1016/j.isci.2023.107431>



Table 1. Arena specifications across time points

Age	7 dpf	28 dpf	42 dpf	70 dpf
Arena (diameter x depth) (mm)	96 x 7	177 x 7	242 x 25	339 x 25

Arena diameters and depths, in mm, for each Arena diameters and depths, in mm, for each time point assayed.

between surface and cave fish provide an opportunity to investigate how individual interactions are altered over evolutionary time to produce differences in group behaviors.

Here, we quantify group dynamics and individual behaviors in groups of cave and surface *A. mexicanus* across ontogeny to identify how changes in individual fish behaviors lead to evolutionary loss of collective motion. By examining inter-individual interactions across development, we are able to identify when during development fish initially begin to modulate their motion relative to their neighbors, and how these changes in individual behaviors alter group level behaviors. Through comparing inter-individual interactions across populations that exhibit markedly different group level behaviors, we define how different social interaction rules underlying group behaviors have evolved, as well as when the developmental trajectories leading to different group level behaviors diverge.

RESULTS

Attraction and alignment diverge between surface and cave fish over the course of development

The ontogeny of schooling and shoaling in surface fish, as well as the stage at which cave and surface fish social behaviors diverge, is unknown. For example, surface and cave fish may display distinct social interactions throughout development. Alternatively, they may initially display similar interactions before diverging later in development. To determine if schooling and shoaling change across development (Table 1), we analyzed swimming behavior in surface fish and cave fish in groups of five at timepoints across development: 7 days post fertilization (dpf) (n = 7 surface fish groups and 11 cave fish groups), shortly after fish begin to hunt prey and feed, 28 dpf (n = 8 surface fish groups and 9 cave fish groups), 42 dpf (n = 9 surface fish groups and 7 cave fish groups), and 70 dpf (n = 11 surface fish groups and 9 cave fish groups), when fish have reached subadult stages, but prior to sexual maturity. We calculated the distance (Figure 1A) and the alignment (Figure 1B) between pairs of fish, as these metrics have previously been used to define schooling and shoaling^{11,22,53,54} (Figure 1C). The joint probability distributions of pair distance and pair angle spread over the entire range of distances and angles in surface *A. mexicanus* at larval and juvenile time points (7 and 28 dpf; Figures 1D and 1E), suggesting that surface fish at these stages of development are neither schooling nor shoaling. However, while the pair distances and angles continue to spread across the entire range at 42 dpf, by this point in development the distribution also exhibits a peak at short pair distance and small pair angle, suggesting some preference for proximity and alignment by this stage (Figure 1F). In groups of 70 dpf surface fish, the joint probability distribution of pair distance and angle has a sharp peak at short pair distances, which is more pronounced at small pair angles, suggesting that surface fish show a strong preference for proximity and alignment at this stage (Figure 1G). These 70 dpf results indicate that fish are schooling and shoaling at this stage. Together these data suggest that in surface fish, schooling and shoaling emerge over the course of development, with an initial preference for being both aligned and in close proximity beginning prior to 42 dpf and becoming robust by 70 dpf.

To determine if evolutionary loss of schooling in cavefish occurs at late developmental stages, or if surface and cave fish behavioral differences in sociality can be observed throughout developmental stages, we assessed whether cave fish demonstrate a preference for alignment and proximity at any point in development. Similar to surface fish at the same stages, the joint probability distributions of pair distance and pair angle for 7 dpf and 28 dpf cave fish groups spread over the entire available range of distances and angles (Figures 1H and 1I). However, while surface fish begin to exhibit patterns of inter-fish proximity and alignment associated with schooling and shoaling at 42 dpf, cave fish do not. Instead, the joint probability distribution of pair distance and pair angle continues to spread over a range of distances and angles in 42 dpf and 70 dpf cave fish groups, suggesting a lack of preference for proximity or alignment at these later developmental stages (Figures 1J and 1K). A different pattern emerges in 70 dpf cave fish: a pair of arches that suggests a strong preference for swimming along the arena walls (Figure 1K).⁵³ These findings suggest that cave fish do not school or shoal at any point in development. Taken together, these results

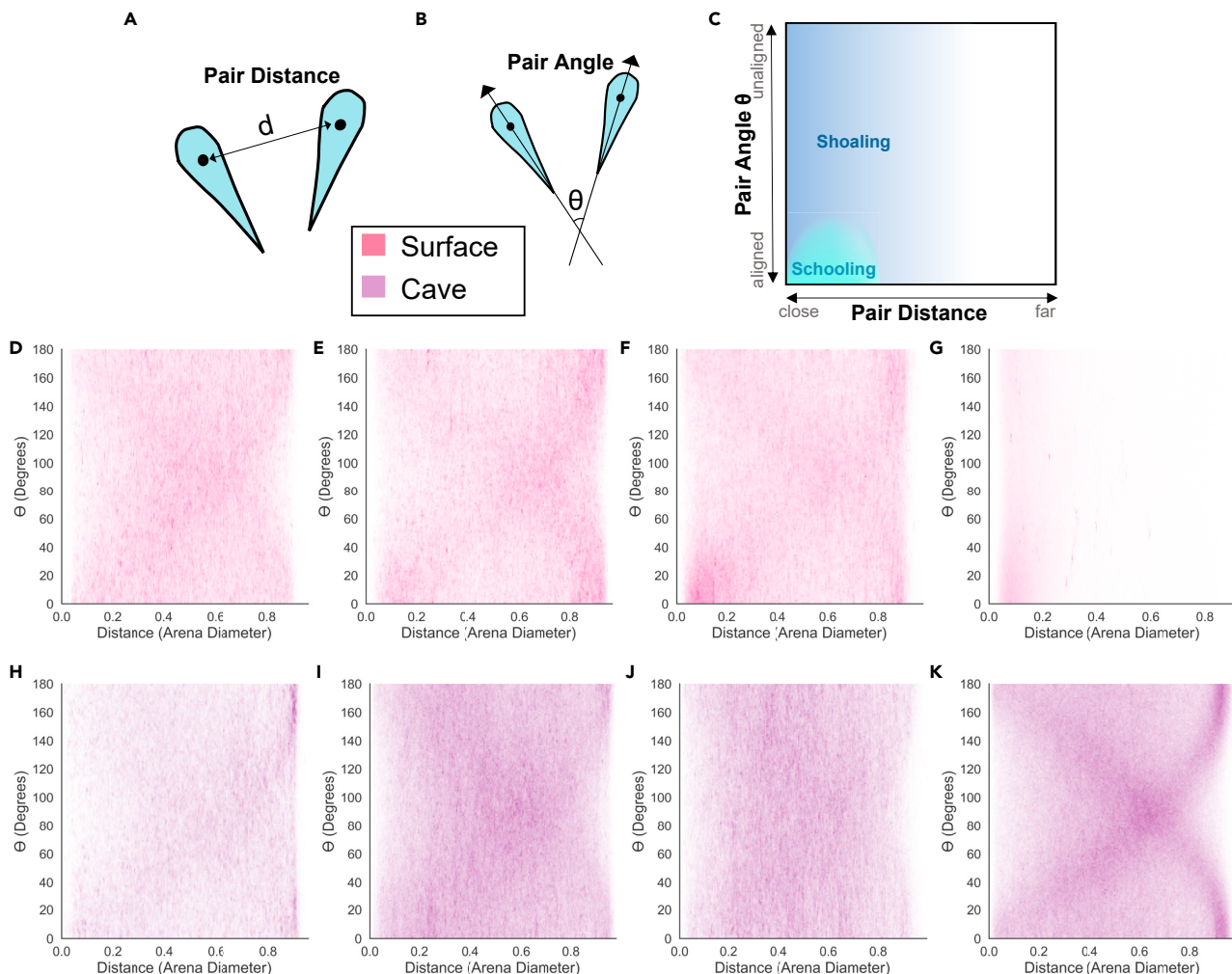


Figure 1. Joint probability distributions of pair distance and angle between individuals in groups of five fish

- (A) Pair distance was defined as the distance between the center points of two individuals.
- (B) Pair angle was defined as the difference in heading between two individuals.
- (C) Collective behaviors such as schooling and shoaling can be broadly defined using the relationship between pair distance and angle.
- (D–G) Joint plots for groups of surface fish at (D) 7 dpf, (E) 28 dpf, (F) 42 dpf, and (G) 70 dpf.
- (H–K) Joint plots for groups of cave fish at (H) 7 dpf, (I) 28 dpf, (J) 42 dpf, or (K) 70 dpf.

indicate that the attraction and alignment that underlie schooling behavior emerge in surface fish over the course of development, with attraction and/or alignment being present at 42 dpf, and that these behaviors do not follow this developmental trajectory in cavefish.

Surface fish develop the tendency to align prior to attraction

We next asked if attraction and tendency to align to neighbors are established at the same developmental stages in surface fish. To determine when in development surface fish begin to exhibit a preference for alignment to one another, we compared the angles of fish to their nearest neighbors across ontogeny. To control for indirect alignment, e.g., fish being aligned because they are following the same wall rather than because they are reacting to each other's presence, the alignment of nearest neighbors was compared to the alignment of nearest neighbors in mock groups, a frequently used approach.^{18,20,50,55} Mock groups were generated by extracting the positions of individuals that were not assayed together and combining them to form groups of five fish (see STAR Methods). At 7 dpf, surface fish nearest neighbor alignment was similar to mock groups ($p = 0.097$; Figures 2A and S1), suggesting that at early stages of development, surface fish do not have a preference for alignment. Beginning at 28 dpf, however, there

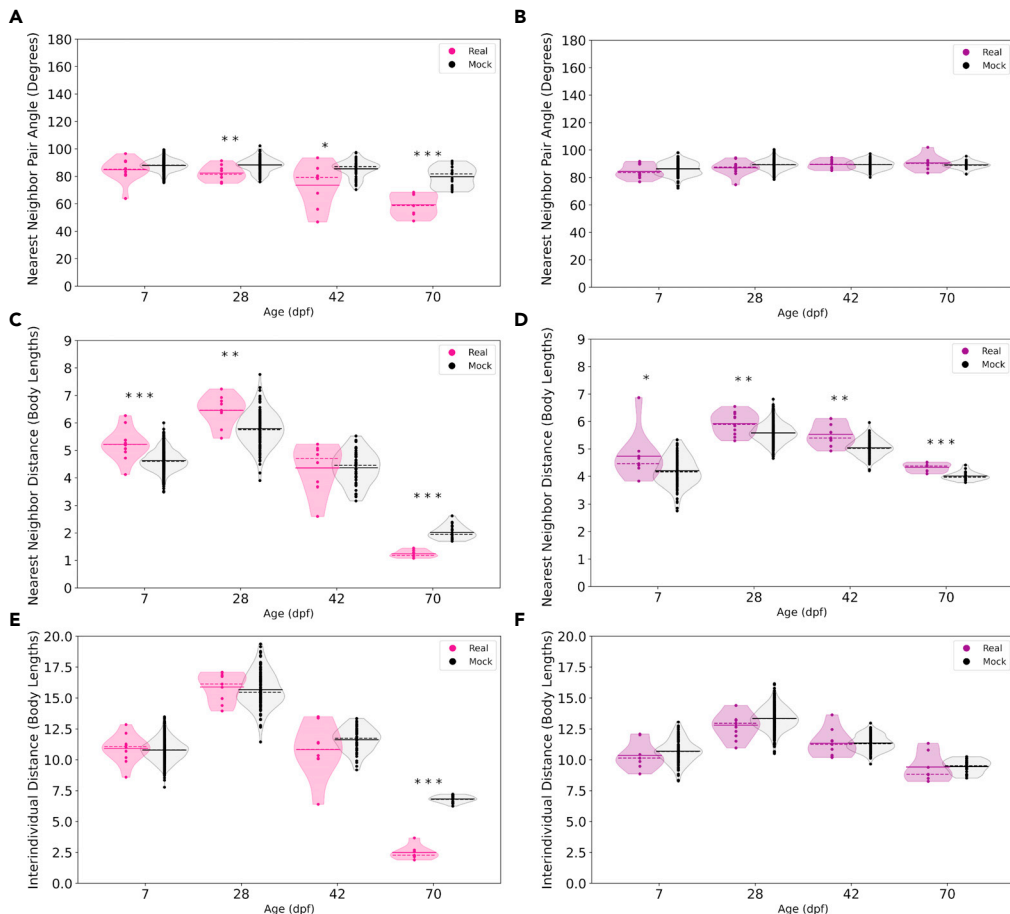


Figure 2. Comparisons of surface and cave fish proximity and alignment to that of mock groups

(A and B) (A) Comparisons of surface fish (left violin plots, pink) nearest neighbor pair angles to mock groups (right violin plots, gray) at 7 dpf ($p = 0.097$), 28 dpf ($p = 0.004$), 42 dpf ($p = 0.016$), and 70 dpf ($p < 0.001$) (B) Comparisons of cave fish (left violin plots, purple) nearest neighbor pair angle to mock groups (right violin plots, gray) at 7 dpf ($p = 0.246$), 28 dpf ($p = 0.126$), 42 dpf ($p = 0.954$), and 70 dpf ($p = 0.568$).

(C) Comparisons of surface fish nearest neighbor distances to mock groups at 7 dpf ($p < 0.001$), 28 dpf ($p = 0.003$), 42 dpf ($p = 0.654$), and 70 dpf ($p < 0.001$).

(D) Nearest neighbor distances of cave fish compared to mock groups at 7 dpf ($p = 0.045$), 28 dpf ($p = 0.008$), 42 dpf ($p = 0.001$), and 70 dpf ($p < 0.001$).

(E) Comparisons of surface fish interindividual distance to mock groups at 7 dpf ($p = 0.490$), 28 dpf ($p = 0.534$), 42 dpf ($p = 0.257$), and 70 dpf ($p < 0.001$).

(F) Interindividual distances in groups of cave fish compared to mock groups at 7 dpf ($p = 0.162$), 28 dpf ($p = 0.091$), 42 dpf ($p = 0.587$), and 70 dpf ($p = 0.499$). Solid lines denote means, dotted lines denote medians, each point denotes a single trial, * denotes $p < 0.05$, ** denotes $p < 0.01$, *** $p < 0.001$, $\alpha = 0.05$. See Figure S1 for full table of statistics. P-values here are the result of Mann-Whitney U-tests.

is a statistically significant decrease in pair angle in actual groups of surface fish compared to pair angle in mock groups ($p = 0.004$; Figures 2A and S1), indicating that fish aligned more with their neighbors than expected by chance. At 42 dpf and 70 dpf, alignment between nearest neighbors relative to alignment in mock groups became more pronounced than at earlier developmental timepoints (42 dpf: $p = 0.016$; 70 dpf: $p < 0.001$; Figures 2A and S1), suggesting that in surface fish, the tendency to align with nearest neighbors becomes more pronounced over the course of development. In contrast, the alignment of nearest neighbors in groups of cave fish did not significantly differ from the alignment of mock group nearest neighbor pairs at any of the developmental timepoints (7 dpf: $p = 0.246$; 28 dpf: $p = 0.126$; 42 dpf: 0.954 ; 70 dpf: $p = 0.568$; Figures 2B and S1). Importantly, the nearest neighbor pair angles of surface and cave fish did not strongly correlate with swimming speed at any developmental stage, suggesting

the observed trends are not simply the consequence of differences in swimming speed (Figures S2A and S2B). Together, these data suggest that a preference to align with neighbors emerges between 7 dpf and 28 dpf in surface fish and increases over time. By contrast, cave fish demonstrate no tendency to align with neighbors at any timepoint, suggesting that loss of tendency to align contributes to loss of schooling in cavefish.

In addition to alignment, attraction to others in the group is essential for schooling and shoaling behavior in fish. To determine when fish first begin to show attraction to other fish in the group, we calculated two commonly used metrics of attraction: nearest neighbor distance, the distance between each fish and its closest neighbor, and interindividual distance, the distances between all pairs of fish in the group, a measure of group cohesion. Nearest neighbor distances and interindividual distances of real groups were compared to those of the same mock groups used for alignment comparisons. At 7 dpf and 28 dpf, surface fish nearest neighbor distances were significantly larger than those of mock groups (7 dpf $p < 0.001$; 28 dpf $p = 0.003$, Figures 2C and S1). This changes at 42 dpf, when surface fish nearest neighbor distances were similar between real and mock groups ($p = 0.654$; Figures 2C and S1). By 70 dpf, however, surface fish maintained significantly closer nearest neighbor distances compared to mock groups ($p < 0.001$; Figures 2C and S1). These data suggest that surface fish do not display attraction during early development, and may avoid neighbors at these developmental stages. Further, they suggest that surface fish begin to display robust attraction by 70 dpf. This establishment of attraction by 70 dpf is also observed at the level of group cohesion. At 7, 28, and 42 dpf, surface fish interindividual distances resembled those of mock groups (7 dpf $p = 0.490$; 28 dpf $p = 0.534$; 42 dpf 0.257 ; Figures 2E and S1). However, at 70 dpf, surface fish groups show cohesiveness, with interindividual distances that are significantly smaller compared to mock groups ($p < 0.001$; Figures 2E and S1).

Across development, cave fish maintained significantly greater distances from their nearest neighbors compared to mock groups (7 dpf: $p = 0.045$; 28 dpf: $p = 0.008$; 42 dpf: $p = 0.001$; 70 dpf: $p < 0.001$; Figures 2D and S1). However, the interindividual distances in groups of cave fish resembled those of control mock groups over the course of all developmental timepoints assayed (7 dpf: $p = 0.162$; 28 dpf: $p = 0.091$; 42 dpf: $p = 0.587$; 70 dpf: $p = 0.499$; Figures 2F and S1). These data suggest that cave fish do not exhibit attraction to neighbors at any point in development, and may exhibit repulsion from nearest neighbors. We found no strong correlations between swimming speed and nearest neighbor distance or interindividual distance in surface fish or cave fish at most stages, except at 70 dpf where it correlated with approximately 20% of the variability observed in interindividual distance in cave fish, suggesting the observed trends are not simply the consequence of differences in swimming speed (Figures S2A and S2B). Taken together, these data suggest that surface fish attraction and preference for alignment develop at distinct points in development, and that lack of a preference for alignment or attraction is maintained in cavefish across ontogeny.

Reductions in tendency to modulate speed and turning according to neighbor position underlie loss of schooling in cave fish

We next sought to understand how fish modulate the ways they interact with their neighbors to give rise to the emergence of schooling and shoaling, and how these inter-fish interactions differ between populations that have evolved differences in the tendency to school and shoal. We first defined inter-fish positional preferences by generating density heat maps around a focal fish and looking for differences between real groups of fish and mock groups. At 70 dpf, when surface fish school and shoal, they exhibit specific positional preferences relative to neighboring fish when compared to mock groups: Fish are frequently positioned such that neighboring fish occupy a zone between 0.05 and 0.4 tank radii from a focal fish, a zone we refer to as the schooling zone (Figures 3A and S3A). In contrast, fish in 70 dpf surface fish mock groups do not preferentially occupy the schooling zone (Figure S4A). This positional preference is also observed, to a lesser extent, at 42 dpf (Figure 3A). However, it is not present at earlier developmental stages. Instead, density maps of 7 and 28 dpf surface fish indicate low fish density at close distances relative to the focal fish (Figure 3B). Together, these data suggest that neither surface nor cave fish display robust attraction early in development, however surface fish develop attraction over the course of development, consistent with the emergence of schooling behavior in these fish.

Fish can modulate their position relative to neighbors using a combination of two behaviors: turning and changing swimming speed, and one or both of these behaviors could be altered by evolution in cave fish. In

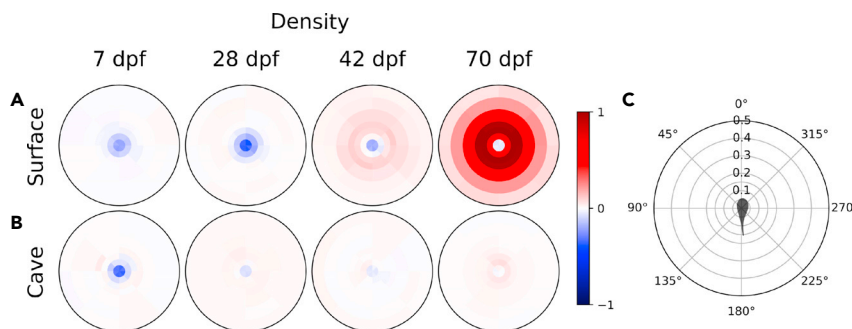


Figure 3. Positional preferences of surface and cave fish across development compared to mock groups

(A and B) Density heat maps illustrate the preferred positions of (A) surface and (B) cave fish individuals relative to a focal fish located at the center of the heatmap, facing upwards. Results are the difference between real (Figure S3) and mock groups of 5 fish (Figure S4). Positive values (red) indicate that the presence of a neighbor is more likely in real groups than in mock groups. Negative values (blue) indicate that the presence of a neighbor is less likely in real groups than in mock groups.

(C) Polar grid. The focal fish is shown in the center, facing up. The rings at 0.05, 0.1, 0.15, 0.2, 0.3, 0.4, and 0.5 tank radii show the distance between the focal fish and its neighbor.

order to determine the contributions of speed changes and turning to the maintenance of preferred positions, we computed the average speeding and turning forces of each fish when another fish is nearby as a function of the neighboring fish's location, similar to previous work in golden shiners.¹¹ Force here refers to the focal fish's acceleration normalized to average speed. The turning force is the normal acceleration (acceleration perpendicular to the fish's heading). The speeding force is the tangential acceleration (acceleration in the direction of the fish's heading). In order to control for the effects of arena walls, speeding and turning force were also calculated for individuals in mock groups, and the difference between real (Figures S3C–S3F) and mock group data (Figures S4C–S4F) were plotted as heat maps (Figures 4A, 4B, 5A, and 5B). At 70 dpf, surface fish tend to increase swimming speed if a neighbor is located further than ~0.15 tank radii in front of them and decrease swimming speed if a neighbor is located further than ~0.15 tank radii behind them (Figure 4A). Since 0.15 tank radii corresponds to the peak of the neighbor density heatmap (Figure 3A), this suggests that 0.15 tank radii is the preferred distance between schooling neighbors, and that fish modulate their speed to get closer to their neighbor when that neighbor is further away than this preferred distance.

In order to quantitatively assess the contribution of speed changes to attraction, we calculated the mean attractive speeding force for all pairs of fish within the attraction zone, defined as the region between 0.15 and 0.4 tank radii of a focal fish, i.e., the part of the schooling zone where the speeding force is expected to be attractive (Figure 4C). Positive values indicate that speed changes tend to decrease the distance between neighbors whereas negative values indicate that speed changes tend to increase the distance between neighbors. Values close to zero indicate that individuals are not utilizing changes in swimming speed to change their distance relative to neighbors. To account for speeding due to non-social effects, we subtracted the mock group mean from the mean of each real group. At 70 dpf, the mean trial attractive speeding force of surface fish is significantly greater than zero ($p = 0.002$), indicating that fish show a tendency to use speed to position themselves closer to neighbors at this stage (Figure 4D and S5). At 7, 28 and 42 dpf, surface fish do not appear to modulate speed in response to neighbors in the attraction zone, and mean trial attractive speeding forces do not differ significantly from zero (7 dpf $p = 0.151$; 28 $p = 0.606$; 42 dpf $p = 0.091$) (Figures 4A, 4D, and S5).

Cave fish attractive speeding force did not significantly differ from zero at 7 dpf ($p = 0.115$) or 42 dpf ($p = 0.820$), although speeding force was slightly greater than zero at 28 dpf ($p = 0.014$) (Figures 4E and S5). Unlike in surface fish, cave fish speeding forces at 70 dpf ($p = 0.109$) also did not differ from zero (Figures 4E and S5), consistent with the positional preferences and observed lack of schooling and shoaling at these stages. Considering the similarities in surface and cave fish positional preferences at early stages (Figures 3A and 3B), we hypothesized that surface and cave fish may exhibit similar trends in speeding force at close proximities during this stage. Within close proximities, surface fish at 7 and 28 dpf slow down when fish are in front of them and speed up when fish are behind them, a trend that continues across time points and is present in cave fish (Figures 4A and 4B). Together, these data suggest that both surface and cave fish alter their speed to maintain positional

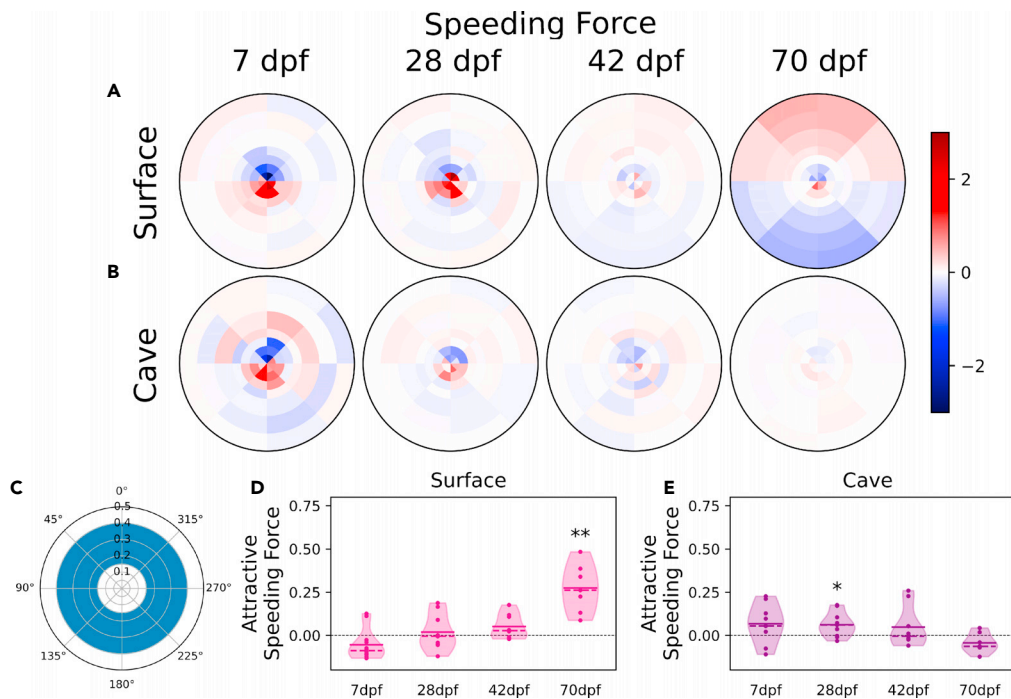


Figure 4. Fish modulate swimming speed according to the relative position of neighbors

(A and B) Speeding force represents the acceleration of an individual (A) surface or (B) cave fish in the axis of its motion. Speeding force here is given as a function of the position of neighboring fish, with the focal fish's direction of motion oriented toward the top of the figure. Positive values (red) indicate increases in swimming speed. Negative values (blue) indicate decreases in swimming speed.

(C) The mean speeding force for each trial was calculated for pairs within proximities in which attraction was expected (0.15 and 0.4 tank radii) and its sign flipped when the neighboring fish was behind the focal fish to give the attractive speeding force. Positive values indicate that speed changes tend to decrease the distance between neighbors whereas negative values indicate that speed changes tend to increase the distance between neighbors.

(D) The mean attractive speeding forces of surface fish at 7 dpf ($p = 0.151$), 28 dpf ($p = 0.606$), 42 dpf ($p = 0.091$), and 70 dpf ($p = 0.002$).

(E) The mean attractive speeding forces of cave fish at 7 dpf ($p = 0.115$), 28 dpf ($p = 0.014$), 42 dpf ($p = 0.820$), and 70 dpf ($p = 0.109$). Accelerations here have been standardized to mean swimming speed of each age and population. * denotes $p < 0.05$, ** denotes $p < 0.01$, $\alpha = 0.05$. Results here are the difference between real and mock data. See Figure S5 for full table of statistics. P-values here are the result of either a one sample t-tests or a Wilcoxon Signed Rank test. See STAR Methods and Figure S5 for more information.

preferences relative to neighbors, but only surface fish develop the tendency to modulate speed to get closer to neighbors, contributing to maintenance of close proximity required for schooling and shoaling.

Next, we assessed whether fish modulate their position relative to other fish through turning. Surface fish at 70 dpf turn toward neighbors located any greater than 0.15 tank radii to the right or left of them (Figure 5A). Similar to speeding force, we calculated the attractive turning force (positive if the turn is toward neighbor, negative if it's away from it) averaged over every pair of fish within the attraction zone (Figure 5C). To account for turning due to non-social effects, we subtracted the mock group mean from the mean of each real group. At 70 dpf, the attractive turning force in surface fish is significantly higher than zero ($p = 0.002$) (Figures 5D and S6). A slight tendency to turn toward neighbors can be observed in heat maps at 42 dpf, and an attractive turning force slightly higher than zero, though the difference was not statistically significant ($p = 0.072$; Figures 5A, 5D, and S6). Turning toward neighbors is not observed in 7 ($p = 0.698$) or 28 dpf surface fish ($p = 0.331$; Figures 5A, 5D, and S6). Similar to trends observed in speeding force, both surface fish and cave fish turn away from fish located within ~ 0.1 tank radii across development (Figures 5A and 5B). However, the attractive turning force of cave fish did not significantly differ from zero, except at 28 dpf (7 dpf $p = 0.820$; 28 dpf $p = 0.018$; 42 dpf $p = 0.139$; 70 dpf $p = 0.094$; Figures 5E and S6). Taken together, these findings indicate that surface and cave fish utilize both speeding and turning to maintain preferred positions to neighbors, but only in surface fish during later developmental stages is

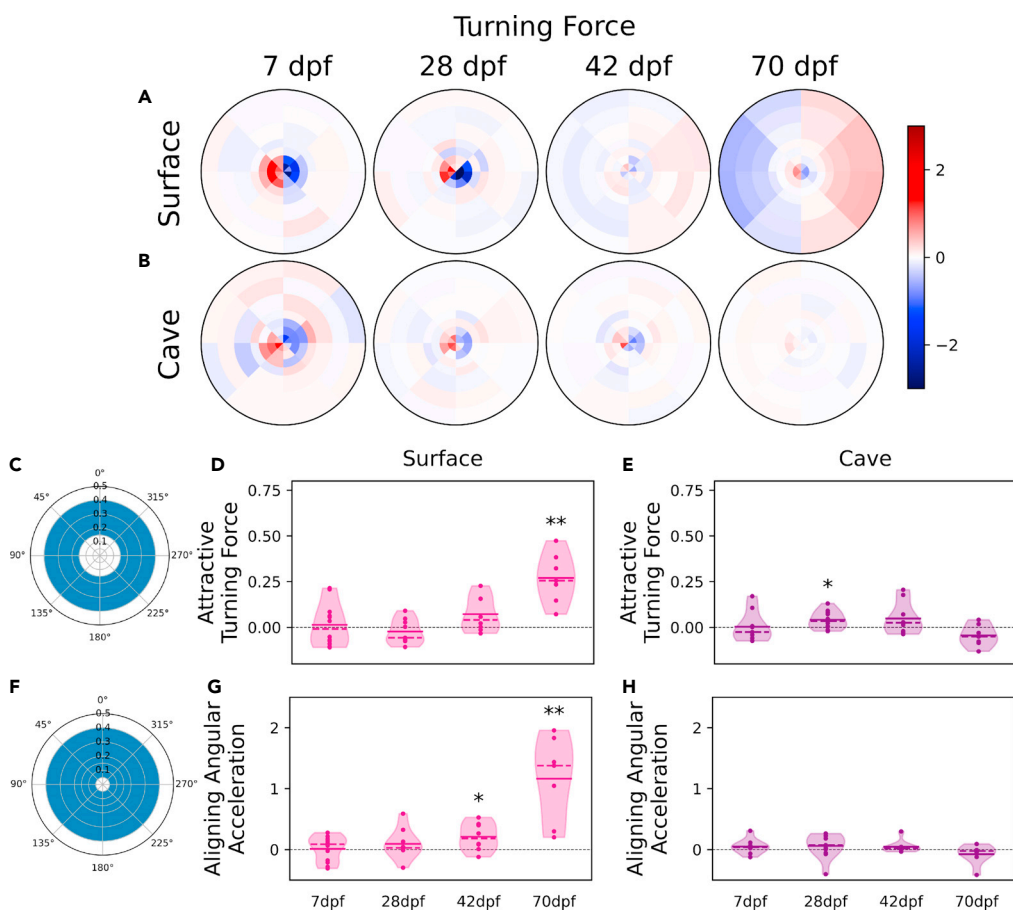


Figure 5. Fish perform turns to control alignment and proximity to neighbors

(A and B) Turning force represents acceleration perpendicular to a focal (A) surface or (B) cave fish's axis of motion. Turning force here is given as a function of the position of neighboring fish, with the focal fish's direction of motion oriented toward the top of the figure. Positive values (red) indicate acceleration to the right. Negative values (blue) indicate acceleration to the left.

(C) The mean turning force for each trial was calculated for pairs within the attraction zone and its sign flipped when the neighboring fish was on the left side of the focal fish to get the attractive turning force. Positive values indicate turning toward a neighbor and negative values indicate turning away.

(D) Mean attractive turning forces of surface fish at 7 dpf ($p = 0.698$), 28 dpf ($p = 0.331$), 42 dpf ($p = 0.072$), and 70 dpf ($p = 0.016$) compared to zero.

(E) Mean attractive turning forces of cave fish at 7 dpf ($p = 0.820$), 28 dpf ($p = 0.018$), 42 dpf ($p = 0.139$), and 70 dpf ($p = 0.094$) compared to zero.

(F) The contribution of turning to maintaining alignment with neighbors was assessed by comparing the mean trial angular acceleration of pairs within 0.05 and 0.4 tank radii of each other (see [STAR Methods](#)).

(G) Mean angular accelerations of surface fish at 7 dpf ($p = 0.831$), 28 dpf ($p = 0.280$), 42 dpf ($p = 0.035$), and 70 dpf ($p = 0.004$) compared to zero.

(H) The mean angular acceleration of cave fish did not differ from zero at 7 dpf ($p = 0.247$), 28 dpf ($p = 0.329$), 42 dpf ($p = 0.055$), or 70 dpf ($p = 0.156$). Accelerations here have been standardized to mean swimming speed of each age and population. * denotes $p < 0.05$, ** denotes $p < 0.01$, $\alpha = 0.05$. Results here are the difference between real and mock data. See [Figure S6](#) for full table of statistics. P-values here are the result of either a one sample t-tests or a Wilcoxon Signed Rank test. See [STAR Methods](#) and [Figure S6](#) for more information.

turning utilized to maintain closer proximities to neighbors. This suggests that the evolved loss of schooling in cave fish is the product of a loss of these attractive trends in both speeding and turning.

Fish may utilize turning to alter both their proximity and their alignment relative to other individuals. In order to assess the contribution of turning to the tendency of fish to align with neighbors we calculated the aligning angular acceleration of neighbors located within 0.05–0.4 tank radii of each other (see [STAR](#)

Methods; Figure 5F). The aligning angular acceleration was calculated as the rate of change of the angular velocity, with a minus sign when the neighbor is on the left of the focal fish so that positive values always correspond to an effort (a torque) to align with the neighbor's heading whereas negative values indicate an effort to turn away from the neighbor's heading. At both 42 dpf ($p = 0.035$) and 70 dpf ($p = 0.004$), surface fish angular acceleration is significantly higher than zero, indicating that turning contributes significantly to surface fish tendency to align with neighbors at these ages (Figures 5G and S6). In contrast, the angular acceleration of cave fish was close to zero across development, suggesting that fish neither turned to align nor to misalign with neighbors (7 dpf $p = 0.247$; 28 dpf $p = 0.329$; 42 dpf $p = 0.055$; 70 dpf $p = 0.156$; Figures 5H and S6). Taken together, these results indicate that at late stages of development in surface fish, turning contributes to a preference for being aligned, whereas cave fish have evolved a reduced tendency to turn to align to neighbors.

DISCUSSION

Collective motion is a complex emergent property that arises from interactions between individuals at the local level.^{11,15–17,56–60} Schooling and shoaling in fish are examples of collective motion, and while the local interactions that underlie schooling and shoaling have been studied in several fish species,^{11,15,16} little is known about how natural variation in these local interactions result in evolved differences at the level of the emergent collective behavior.⁹ There is considerable variation in schooling and shoaling among fish that live in different ecological conditions. For example, populations of Trinidadian guppies display different degrees of group cohesion, and cohesiveness positively correlates with the degree of predation in their natural habitats.^{12,17,21,61–63} Additionally, sociality of three-spine stickleback populations varies according to water temperature during rearing – a trend that is particularly worrisome as global temperatures rise.⁶⁴ While there is significant diversity in the tendency to school and shoal across populations of fishes, how evolution impacts local interaction rules to produce these group level differences is not understood. Here, we illustrate how evolved changes in interindividual interactions culminate in the development of naturally occurring differences in schooling and shoaling in closely related populations of a single species.

While studies in zebrafish have laid the groundwork for understanding how complex collective behaviors manifest over the course of development, *A. mexicanus* represents a unique opportunity to not only determine how collective behaviors emerge over development, but also how the individual behaviors and pairwise interactions that underlie collective motion change when emergent behaviors evolve. Cave *A. mexicanus* exhibit reductions in schooling similar to those of other cave fish, such as cave mollies (*Poecilia mexicana*)^{15,65–67} and cave Oman garra (*Garra barreimiae*).⁶⁸ Observations of differences in the collective behaviors of adult surface and cave populations of the Mexican tetra go back at least as far as 1964,⁵¹ and include both field and lab studies.^{49,51–53} However, it was only recently that studies began capitalizing on automated tracking, allowing for previously unattainable in-depth quantitative analysis of these behaviors.^{50,53} These studies demonstrate that, although they do not exhibit robust schooling and shoaling, adult cave fish modulate their behavior in the presence of conspecifics by altering average swimming and turning speeds, and that their sociality may be altered by environmental conditions.^{50,53} Thus, cave fish present an opportunity to understand mechanisms contributing to evolution of collective behaviors. Here, we assess differences in how individual fish respond to other individuals in these populations of schooling and non-schooling fish. We find that by 70 dpf, the collective behaviors of surface and cave fish resemble those of adults of the same populations assayed under similar conditions,⁵³ with surface fish exhibiting schooling and cave fish displaying no attraction or tendency to align. Further, we have characterized the individual level behavioral changes that underlie these differences in schooling and shoaling: Surface fish utilize turning and changes in speed to maintain close proximities and alignment relative to neighbors, similar to individuals from other schooling species.^{11,16,18} Changes in swimming speed are utilized by surface fish to control proximity to neighbors, while turning is utilized to control both proximity and alignment to neighbors. In contrast, while cave fish also utilize turning and speed changes to control their positions relative to neighbors, they do not appear to utilize turning to alter their alignment relative to neighbors. Furthermore, cave fish only perform turns and modulate speed to separate from neighbors, they do not perform turns or modulate speed to maintain close proximities to neighbors, resulting in the loss of the robust attraction and alignment found in schooling and shoaling fish. Similarly, experiments in which groups of guppies were artificially selected for greater group alignment across multiple generations also resulted in changes in the relationship between both turning and changes in speed relative to the positions of neighbors.⁶⁹ Groups selected for greater cohesion exhibited stronger correlations between turning and nearest neighbor direction. The correlation between turning and nearest neighbor position in groups selected for cohesion was not significantly stronger than in non-selected groups, though a slight trend was

observed.⁶⁹ These findings, along with our results in *A. mexicanus*, support the idea that the modulation of turning and speed is essential to evolved differences in collective behavior across fish species.

One approach for understanding how changes at the level of local interactions affect schooling and shoaling is to perform in-depth quantitative analyses of the interactions across developmental timepoints. To the best of our knowledge, analyses of the development of schooling and shoaling had exclusively been conducted in the zebrafish, *Danio rerio*, prior to this study.^{18,20,70} Similar to our findings in the Mexican tetra, zebrafish develop attraction and tendency to align to other fish at distinct points in development.^{18,20,70} Interestingly, previous genetic screens indicate that attraction and alignment for schooling and shoaling are regulated by different genes.⁵⁴ While the exact timing of the onset of attraction and alignment differ between studies, all of the proposed times of onset are earlier than in *A. mexicanus*. Similar to our results in surface *A. mexicanus*, developmental changes in tendency to align and attraction in zebrafish are the product of changes in the ways individual fish modify their velocity in response to neighbors.¹⁸ Whether the differences in ontogeny of schooling across species are due to life history or differences in ecological factors under which these populations have evolved remains an open question.

Analysis of ontogeny of schooling and shoaling in cave and surface fish revealed similarities between the inter-individual interactions of fish from both populations early in development. In addition to similar trends in nearest neighbor pair angle, interindividual distance, and nearest neighbor distance when compared to control mock data at early stages of development, analysis of individual behaviors relative to neighbors suggests that both cave fish and surface fish modulate speed and turning to create distance between themselves and close neighbors, and do not modulate speeding or turning in response to more distant neighbors at early developmental stages, including those in the area that makes up the attraction zone at later stages of development in surface fish. Beginning around 42 dpf, however, the developmental trajectories of these behaviors diverge between surface and cave fish. Surface fish begin to develop robust attractive interactions, turning toward neighbors and modulating speed to remain close to neighbors, as well as aligning interactions, turning to align with neighbors. Neither attraction nor alignment are observed in cavefish, which do not turn nor speed to get closer to or align with neighbors. These data suggest that the evolution of collective behaviors is driven by changes in patterns of speeding and turning by individuals to move closer to or align with neighbors.

The lack of differences in social interactions between surface fish and cave fish at early developmental stages suggests a model for how schooling and shoaling evolve: through a loss of behaviors that result in attraction and alignment, rather than loss in all modulation of behavior based on location of other fish. These results, combined with recent advances in *A. mexicanus* research, including Tol2 transgenesis,⁷¹ CRISPR gene editing,³⁹ and neuroanatomical brain atlases,^{72–74} will provide a unique opportunity to probe for the neuronal and genetic mechanisms underlying naturally occurring variation in components of collective behavior in future studies.

Multiple traits differ between surface and cave fish both early in development and at adult stages, including reductions in sleep^{38,75} and reduced stress-associated behaviors.^{37,76} Other traits diverge over the course of ontogeny. For example, studies investigating developmental differences between populations have revealed that larval cave fish initially develop eyes that then regress.^{77–81} However, cavefish eyes still exhibit a number of differences during early developmental stages compared to surface fish eyes,⁷⁸ and cavefish likely lack functional vision even early in development, as they do not respond to visual stimuli and show defects in photoreceptor development.^{82,83} Thus, the emergence of differences in social behavior across development is distinct from some cave-evolved traits.

Collective behaviors are exhibited by a wide variety of animals and, like schooling and shoaling in fishes, are the product of local interactions between individuals.^{15–17,56–60} Indeed, this trend applies not only to animals but also to groups of cells or even moving particles.^{84–88} Understanding the mechanisms underlying collective behaviors may have wide applications. For example, the collective behaviors of fish have been used as models for underwater robot swarms, which may be used for applications in environmental monitoring.⁸⁹ The collective behaviors of termites have also been used as models for designing groups of robots that build user-specified structures.⁹⁰ Thus, the ability to understand how changes in local interactions influence collective behaviors is relevant to a wider variety of disciplines than simply animal behavior, emphasizing the significance of data such as those presented here.

Limitations of the study

In this study, we identify developmental timepoints during the emergence of differences between complex social behaviors in populations of the Mexican tetra, *Astyanax mexicanus*. In this work, we did not assess the contributions of differences in sensory perception, which differ between cave fish and surface fish, to the behavioral differences analyzed. Our analysis also focused on pairwise interactions and correlations; we did not assess 3-fish interactions or group-wide effects such as the mean speed's dependence on group size seen in adult cave fish. Additionally, here, we identify points in development using time since fertilization; however, it is possible that differences in husbandry, such as feeding regimen, could result in differences in rate of development and therefore affect the exact time at which the behaviors studied herein emerge over the course of development.

STAR★METHODS

Detailed methods are provided in the online version of this paper and include the following:

- [KEY RESOURCES TABLE](#)
- [RESOURCE AVAILABILITY](#)
 - Lead contact
 - Materials availability
 - Data and code availability
- [EXPERIMENTAL MODEL AND SUBJECT DETAILS](#)
 - Animal care
- [METHOD DETAILS](#)
 - Behavioral experiments
- [QUANTIFICATION AND STATISTICAL ANALYSIS](#)
 - Tracking
 - Mock group formation
 - Orientation and distance analyses
 - Density heatmaps
 - Force heatmaps
 - Attractive speeding and turning force
 - Aligning angular acceleration
 - Density, force, and angular acceleration mock data
 - Statistical analysis of attractive forces and aligning angular acceleration
 - Analysis software

SUPPLEMENTAL INFORMATION

Supplemental information can be found online at <https://doi.org/10.1101/23.107431>.

ACKNOWLEDGMENTS

Funding was provided by National Institutes of Health grant R35GM138345 (JEK), National Science Foundation grant IOS2202359 (J.E.K.) and National Science Foundation EDGE grant 1923372 (J.E.K. and E.R.D.).

AUTHOR CONTRIBUTIONS

Conceptualization: A.P., J.E.K., and Y.F.; Methodology: A.P., J.E.K., and Y.F.; Investigation: A.P., K.J.H., A.C., A.A., B.A., and J.E.K.; Visualization: A.P. and Y.F.; Supervision: J.E.K., Y.F., E.R.D., and A.C.K.; Writing—original draft: A.P. and J.E.K.; Writing—review and editing: A.P., J.E.K., Y.F., E.R.D., A.C.K., K.J.H., A.C., A.A., and B.A.

DECLARATION OF INTERESTS

Authors declare that they have no competing interests.

Received: April 3, 2023

Revised: June 17, 2023

Accepted: July 17, 2023

Published: July 20, 2023

REFERENCES

- Ahmed, I., and Faruque, I.A. (2022). High speed visual insect swarm tracker (Hi-VISTA) used to identify the effects of confinement on individual insect flight. *Bioinspir. Biomim.* 17, 046012. <https://doi.org/10.1088/1748-3190/ac6849>.
- Bialek, W., Cavagna, A., Giardina, I., Mora, T., Silvestri, E., Viale, M., and Walczak, A.M. (2012). Statistical mechanics for natural flocks of birds. *Proc. Natl. Acad. Sci. USA* 109, 4786–4791. <https://doi.org/10.1073/pnas.1118633109>.
- Fullman, T.J., Person, B.T., Prichard, A.K., and Parrett, L.S. (2021). Variation in winter site fidelity within and among individuals influences movement behavior in a partially migratory ungulate. *PLoS One* 16, e0258128. <https://doi.org/10.1371/journal.pone.0258128>.
- Götmark, F., Winkler, D.W., and Andersson, M. (1986). Flock-feeding on fish schools increases individual success in gulls. *Nature* 319, 589–591. <https://doi.org/10.1038/319589a0>.
- Ling, H., McIvor, G.E., van der Vaart, K., Vaughan, R.T., Thornton, A., and Ouellette, N.T. (2019). Local interactions and their group-level consequences in flocking jackdaws. *Proc. Biol. Sci.* 286, 20190865. <https://doi.org/10.1098/rspb.2019.0865>.
- Nagy, M., Akos, Z., Biro, D., and Vicsek, T. (2010). Hierarchical group dynamics in pigeon flocks. *Nature* 464, 890–893. <https://doi.org/10.1038/nature08891>.
- Naidoo, R., Du Preez, P., Stuart-Hill, G., Jago, M., and Wegmann, M. (2012). Home on the Range: Factors Explaining Partial Migration of African Buffalo in a Tropical Environment. *PLoS One* 7, e36527. <https://doi.org/10.1371/journal.pone.0036527>.
- Wang, G., Vega-Rodríguez, J., Diabate, A., Liu, J., Cui, C., Nignan, C., Dong, L., Li, F., Ouedrago, C.O., Bandaogo, A.M., et al. (2021). Clock genes and environmental cues coordinate Anopheles pheromone synthesis, swarming, and mating. *Science* 371, 411–415. <https://doi.org/10.1126/science.abb4359>.
- Greenwood, A.K., Wark, A.R., Yoshida, K., and Peichel, C.L. (2013). Genetic and neural modularity underlie the evolution of schooling behavior in threespine sticklebacks. *Curr. Biol.* 23, 1884–1888. <https://doi.org/10.1016/j.cub.2013.07.058>.
- Ho, J., Plath, M., Low, B.W., Liew, J.H., Yi, Y., Ahmad, A., Tan, H., Yeo, D., and Klaus, S. (2015). Shoaling behaviour in the pygmy halfbeak Dermogenys collettei (Belontiidae: Zenarchopteridae): Comparing populations from contrasting predation regimes. *Raffles Bull. Zool.* 63, 237–245.
- Katz, Y., Tunstrøm, K., Ioannou, C.C., Huepe, C., and Couzin, I.D. (2011). Inferring the structure and dynamics of interactions in schooling fish. *Proc. Natl. Acad. Sci. USA* 108, 18720–18725. <https://doi.org/10.1073/pnas.1107583108>.
- Seghers, B.H. (1974). Schooling Behavior in the Guppy (*Poecilia reticulata*): An Evolutionary Response to Predation. *Evolution* 28, 486–489. <https://doi.org/10.2307/2407174>.
- Suriyampola, P.S., Shelton, D.S., Shukla, R., Roy, T., Bhat, A., and Martins, E.P. (2016). Zebrafish Social Behavior in the Wild. *Zebrafish* 13, 1–8. <https://doi.org/10.1089/zeb.2015.1159>.
- Tang, Z.-H., Wu, H., Huang, Q., Kuang, L., and Fu, S.-J. (2017). The shoaling behavior of two cyprinid species in conspecific and heterospecific groups. *PeerJ* 5, e3397. <https://doi.org/10.7717/peerj.3397>.
- Bierbach, D., Krause, S., Romanczuk, P., Lukas, J., Arias-Rodriguez, L., and Krause, J. (2020). An interaction mechanism for the maintenance of fission–fusion dynamics under different individual densities. *PeerJ* 8, e8974. <https://doi.org/10.7717/peerj.8974>.
- Herbert-Read, J.E., Perna, A., Mann, R.P., Schaefer, T.M., Sumpter, D.J.T., and Ward, A.J.W. (2011). Inferring the rules of interaction of shoaling fish. *Proc. Natl. Acad. Sci. USA* 108, 18726–18731. <https://doi.org/10.1073/pnas.1109355108>.
- Herbert-Read, J.E., Rosén, E., Szarkovszky, A., Ioannou, C.C., Rogell, B., Perna, A., Ramnarine, I.W., Kotrschal, A., Kolm, N., Krause, J., and Sumpter, D.J.T. (2017). How predation shapes the social interaction rules of shoaling fish. *Proc. Biol. Sci.* 284, 20171126. <https://doi.org/10.1098/rspb.2017.1126>.
- Harpaz, R., Nguyen, M.N., Bahl, A., and Engert, F. (2021). Precise visuomotor transformations underlying collective behavior in larval zebrafish. *Nat. Commun.* 12, 6578. <https://doi.org/10.1038/s41467-021-26748-0>.
- Herbert-Read, J.E., Wade, A.S.I., Ramnarine, I.W., and Ioannou, C.C. (2019). Collective decision-making appears more egalitarian in populations where group fission costs are higher. *Biol. Lett.* 15, 20190556. <https://doi.org/10.1098/rsbl.2019.0556>.
- Hinz, R.C., and de Polavieja, G.G. (2017). Ontogeny of collective behavior reveals a simple attraction rule. *Proc. Natl. Acad. Sci. USA* 114, 2295–2300. <https://doi.org/10.1073/pnas.1616926114>.
- Ioannou, C.C., Ramnarine, I.W., and Torney, C.J. (2017). High-predation habitats affect the social dynamics of collective exploration in a shoaling fish. *Sci. Adv.* 3, e1602682. <https://doi.org/10.1126/sciadv.1602682>.
- Jolles, J.W., Boogert, N.J., Sridhar, V.H., Couzin, I.D., and Manica, A. (2017). Consistent Individual Differences Drive Collective Behavior and Group Functioning of Schooling Fish. *Curr. Biol.* 27, 2862–2868.e7. <https://doi.org/10.1016/j.cub.2017.08.004>.
- Tunstrøm, K., Katz, Y., Ioannou, C.C., Huepe, C., Lutz, M.J., and Couzin, I.D. (2013). Collective States, Multistability and Transitional Behavior in Schooling Fish. *PLoS Comput. Biol.* 9, e1002915. <https://doi.org/10.1371/journal.pcbi.1002915>.
- Espinasa, L., Legendre, L., Fumey, J., Blin, M., Rétaux, S., and Espinasa, M. (2018). A new cave locality for *Astyanax* cavefish in Sierra de El Abra, Mexico. *Subterr. Biol.* 26, 39–53. <https://doi.org/10.3897/subterrbiol.26.26643>.
- Herman, A., Brandvain, Y., Weagley, J., Jeffery, W.R., Keene, A.C., Kono, T.J.Y., Bilandžija, H., Borowsky, R., Espinasa, L., O’Quin, K., et al. (2018). The role of gene flow in rapid and repeated evolution of cave related traits in Mexican tetra, *Astyanax mexicanus*. *Mol. Ecol.* 27, 4397–4416. <https://doi.org/10.1111/mec.14877>.
- Jeffery, W.R. (2009). Regressive evolution in *Astyanax* cavefish. *Annu. Rev. Genet.* 43, 25–47. <https://doi.org/10.1146/annurev-genet-102108-134216>.
- Mitchell, R.W., Russell, W.H., and Elliott, W. (1977). Mexican eyeless characin fishes, genus *Astyanax*: Environment, distribution, and evolution. *Spec. Publ. Mus. Tex. Tech Univ* 12, 1–89.
- Boggs, T., and Gross, J. (2021). Reduced Oxygen as an Environmental Pressure in the Evolution of the Blind Mexican Cavefish. *Diversity* 13, 26. <https://doi.org/10.3390/d13010026>.
- Elliott, W.R. (2018). The *Astyanax* Caves of Mexico: Cavefishes of Tamaulipas, San Luis Potosí, and Guerrero (Association for Mexican Cave Studies).
- Fish, E.J. (1977). Karst Hydrogeology and Geomorphology of the Sierra de El Abra and the Valles-San Luis Potosí Region, México.
- Ornelas-García, P., Pajares, S., Sosa-Jiménez, V.M., Rétaux, S., and Miranda-Gamboa, R.A. (2018). Microbiome differences between river-dwelling and cave-adapted populations of the fish *Astyanax mexicanus* (De Filippi, 1853). *PeerJ* 6, e5906. <https://doi.org/10.7717/peerj.5906>.
- Rohner, N., Jarosz, D.F., Kowalko, J.E., Yoshizawa, M., Jeffery, W.R., Borowsky, R.L., Lindquist, S., and Tabin, C.J. (2013). Cryptic Variation in Morphological Evolution: HSP90 as a Capacitor for Loss of Eyes in Cavefish. *Science* 342, 1372–1375. <https://doi.org/10.1126/science.1240276>.
- Tabin, J.A., Aspiras, A., Martineau, B., Riddle, M., Kowalko, J., Borowsky, R., Rohner, N., and Tabin, C.J. (2018). Temperature preference of cave and surface populations of *Astyanax mexicanus*. *Dev. Biol.* 441, 338–344. <https://doi.org/10.1016/j.ydbio.2018.04.017>.
- Alié, A., Devos, L., Torres-Paz, J., Prunier, L., Boulet, F., Blin, M., Eliot, Y., and Rétaux, S. (2018). Developmental evolution of the forebrain in cavefish, from natural variations in neuropeptides to behavior. *Elife* 7, e32808. <https://doi.org/10.7554/elife.32808>.

35. Bibliowicz, J., Alié, A., Espinasa, L., Yoshizawa, M., Blin, M., Hinaux, H., Legendre, L., Pére, S., and Rétaux, S. (2013). Differences in chemosensory response between eyed and eyeless *Astyanax mexicanus* of the Rio Subterráneo cave. *EvoDevo* 4, 25. <https://doi.org/10.1186/2041-9139-4-25>.

36. Borowsky, R. (2016). Chapter 5 - Regressive Evolution: Testing Hypotheses of Selection and Drift. In *Biology and Evolution of the Mexican Cavefish*, A.C. Keene, M. Yoshizawa, and S.E. McGaugh, eds. (Academic Press), pp. 93-109. <https://doi.org/10.1016/B978-0-12-802148-4.00005-0>.

37. Chin, J.S.R., Gassant, C.E., Amaral, P.M., Lloyd, E., Stahl, B.A., Jaggard, J.B., Keene, A.C., and Duboué, E.R. (2018). Convergence on reduced stress behavior in the Mexican blind cavefish. *Dev. Biol.* 441, 319-327. <https://doi.org/10.1016/j.ydbio.2018.05.009>.

38. Duboué, E.R., Keene, A.C., and Borowsky, R.L. (2011). Evolutionary convergence on sleep loss in cavefish populations. *Curr. Biol.* 21, 671-676. <https://doi.org/10.1016/j.cub.2011.03.020>.

39. Klaassen, H., Wang, Y., Adamski, K., Rohner, N., and Kowalko, J.E. (2018). CRISPR mutagenesis confirms the role of oca2 in melanin pigmentation in *Astyanax mexicanus*. *Dev. Biol.* 441, 313-318. <https://doi.org/10.1016/j.ydbio.2018.03.014>.

40. Lloyd, E., Olive, C., Stahl, B.A., Jaggard, J.B., Amaral, P., Duboué, E.R., and Keene, A.C. (2018). Evolutionary shift towards lateral line dependent prey capture behavior in the blind Mexican cavefish. *Dev. Biol.* 441, 328-337. <https://doi.org/10.1016/j.ydbio.2018.04.027>.

41. Protas, M., and Jeffery, W.R. (2012). Evolution and development in cave animals: from fish to crustaceans. *Wiley Interdiscip. Rev. Dev. Biol.* 1, 823-845. <https://doi.org/10.1002/wdev.61>.

42. Yoffe, M., Patel, K., Palia, E., Kolawole, S., Streets, A., Haspel, G., and Soares, D. (2020). Morphological malleability of the lateral line allows for surface fish (*Astyanax mexicanus*) adaptation to cave environments. *J. Exp. Zool. B Mol. Dev. Evol.* 334, 511-517. <https://doi.org/10.1002/jez.b.22953>.

43. Yoshizawa, M., Jeffery, W.R., van Netten, S.M., and McHenry, M.J. (2014). The sensitivity of lateral line receptors and their role in the behavior of Mexican blind cavefish (*Astyanax mexicanus*). *J. Exp. Biol.* 217, 886-895. <https://doi.org/10.1242/jeb.094599>.

44. Breder, C.M. (1943). A Note on Erratic Viciousness in *Astyanax mexicanus* (Phillipi). *Copeia* 1943, 82-84. <https://doi.org/10.2307/1437770>.

45. Burchards, H., Dölle, A., and Parzefall, J. (1985). Aggressive behaviour of an epigean population of *Astyanax mexicanus* (Characidae, Pisces) and some observations of three subterranean populations. *Behav. Processes* 11, 225-235. [https://doi.org/10.1016/0376-6357\(85\)90017-8](https://doi.org/10.1016/0376-6357(85)90017-8).

46. Eliot, Y., Hinaux, H., Callebert, J., and Rétaux, S. (2013). Evolutionary shift from fighting to foraging in blind cavefish through changes in the serotonin network. *Curr. Biol.* 23, 1-10. <https://doi.org/10.1016/j.cub.2012.10.044>.

47. Espinasa, L., Collins, E., Ornelas García, C.P., Rétaux, S., Rohner, N., and Rutkowski, J. (2022). Divergent evolutionary pathways for aggression and territoriality in *Astyanax* cavefish. *Subterr. Biol.* 43, 169-183. <https://doi.org/10.3897/subbiol.73.79318>.

48. Langecker, T.G., Neumann, B., Hausberg, C., and Parzefall, J. (1995). Evolution of the optical releasers for aggressive behavior in cave-dwelling *Astyanax fasciatus* (Teleostei, Characidae). *Behav. Processes* 34, 161-167. [https://doi.org/10.1016/0376-6357\(94\)00063-M](https://doi.org/10.1016/0376-6357(94)00063-M).

49. Gregson, J.N.S., and Burt de Perera, T. (2007). Shoaling in eyed and blind morphs of the characin *Astyanax fasciatus* under light and dark conditions. *J. Fish. Biol.* 70, 1615-1619. <https://doi.org/10.1111/j.1095-8649.2007.01430.x>.

50. Iwashita, M., and Yoshizawa, M. (2021). Social-like responses are inducible in asocial Mexican cavefish despite the exhibition of strong repetitive behavior. *Elife* 10, e72463. <https://doi.org/10.7554/elife.72463>.

51. John, K.R. (1964). Illumination, Vision, and Schooling of *Astyanax mexicanus* (Fillipi). *J. Fish. Res. Bd. Can.* 21, 1453-1473. <https://doi.org/10.1139/f64-122>.

52. Kowalko, J.E., Rohner, N., Rompani, S.B., Peterson, B.K., Linden, T.A., Yoshizawa, M., Kay, E.H., Weber, J., Hoekstra, H.E., Jeffery, W.R., et al. (2013). Loss of schooling behavior in cavefish through sight-dependent and sight-independent mechanisms. *Curr. Biol.* 23, 1874-1883. <https://doi.org/10.1016/j.cub.2013.07.056>.

53. Patch, A., Paz, A., Holt, K.J., Duboué, E.R., Keene, A.C., Kowalko, J.E., and Fily, Y. (2022). Kinematic analysis of social interactions deconstructs the evolved loss of schooling behavior in cavefish. *PLoS One* 17, e0265894. <https://doi.org/10.1371/journal.pone.0265894>.

54. Tang, W., Davidson, J.D., Zhang, G., Conen, K.E., Fang, J., Serluca, F., Li, J., Xiong, X., Coble, M., Tsai, T., et al. (2020). Genetic Control of Collective Behavior in Zebrafish. *iScience* 23, 100942. <https://doi.org/10.1016/j.isci.2020.100942>.

55. Harpaz, R., Aspiras, A.C., Chambule, S., Tseng, S., Bind, M.-A., Engert, F., Fishman, M.C., and Bahl, A. (2021). Collective behavior emerges from genetically controlled simple behavioral motifs in zebrafish. *Sci. Adv.* 7, eabi7460. <https://doi.org/10.1126/sciadv.abi7460>.

56. Ariel, G., Ophir, Y., Levi, S., Ben-Jacob, E., and Ayali, A. (2014). Individual Pause-and-Go Motion Is Instrumental to the Formation and Maintenance of Swarms of Marching Locust Nymphs. *PLoS One* 9, e101636. <https://doi.org/10.1371/journal.pone.0101636>.

57. Ariel, G., and Ayali, A. (2015). Locust Collective Motion and Its Modeling. *PLoS Comput. Biol.* 11, e1004522. <https://doi.org/10.1371/journal.pcbi.1004522>.

58. Corcoran, A.J., and Hedrick, T.L. (2019). Compound-V formations in shorebird flocks. *Elife* 8, e45071. <https://doi.org/10.7554/elife.45071>.

59. Knebel, D., Ayali, A., Guershon, M., and Ariel, G. (2019). Intra- versus intergroup variance in collective behavior. *Sci. Adv.* 5, eaav0695. <https://doi.org/10.1126/sciadv.aav0695>.

60. Young, G.F., Scardovi, L., Cavagna, A., Giardina, I., and Leonard, N.E. (2013). Starling flock networks manage uncertainty in consensus at low cost. *PLoS Comput. Biol.* 9, e1002894. <https://doi.org/10.1371/journal.pcbi.1002894>.

61. Huizinga, M., Ghalambor, C.K., and Reznick, D.N. (2009). The genetic and environmental basis of adaptive differences in shoaling behaviour among populations of Trinidadian guppies, *Poecilia reticulata*. *J. Evol. Biol.* 22, 1860-1866. <https://doi.org/10.1111/j.1420-9101.2009.01799.x>.

62. Magurran, A.E., Seghers, B.H., Carvalho, G.R., and Shaw, P.W. (1997). Behavioural consequences of an artificial introduction of guppies (*Poecilia reticulata*) in N. Trinidad: evidence for the evolution of anti-predator behaviour in the wild. *Proc. R. Soc. Lond. B Biol. Sci.* 248, 117-122. <https://doi.org/10.1098/rspb.1992.0050>.

63. Song, Z., Boenke, M.C., and Rodd, F.H. (2011). Interpopulation Differences in Shoaling Behaviour in Guppies (*Poecilia reticulata*): Roles of Social Environment and Population Origin. *Ethology* 117, 1009-1018. <https://doi.org/10.1111/j.1439-0310.2011.01952.x>.

64. Pilakouta, N., O'Donnell, P.J., Crespel, A., Levet, M., Claireaux, M., Humble, J.L., Kristjánsson, B.K., Skúlason, S., Lindström, J., Metcalfe, N.B., et al. (2023). A warmer environment can reduce sociability in an ectotherm. *Glob. Chang. Biol.* 29, 206-214. <https://doi.org/10.1111/gcb.16451>.

65. Bierbach, D., Lukas, J., Bergmann, A., Elsner, K., Höhne, L., Weber, C., Weimar, N., Arias Rodriguez, L., Mönck, H.J., Nguyen, H., et al. (2018). Insights into the Social Behavior of Surface and Cave-Dwelling Fish (*Poecilia mexicana*) in Light and Darkness through the Use of a Biomimetic Robot. *Front. Robot. AI* 5, 3. <https://doi.org/10.3389/frobt.2018.00003>.

66. Plath, M., and Schlupp, I. (2008). Parallel evolution leads to reduced shoaling behavior in two cave dwelling populations of Atlantic mollies (*Poecilia mexicana*, Poeciliidae, Teleostei). *Environ. Biol. Fishes* 82, 289-297. <https://doi.org/10.1007/s10641-007-9291-9>.

67. Riesch, R., Schlupp, I., Tobler, M., and Plath, M. (2006). Reduction of the Association Preference for Conspecifics in Cave-Dwelling Atlantic Mollies, *Poecilia mexicana*. *Behav. Ecol. Sociobiol.* 60, 794-802.

68. Timmermann, M., Schlupp, I., and Plath, M. (2004). Shoaling behaviour in a surface-dwelling and a cave-dwelling population of a

barb Garra barreimiae (Cyprinidae, Teleostei). *Acta Ethol.* 7, 59–64. <https://doi.org/10.1007/s10211-004-0099-8>.

69. Kotrschal, A., Szorkovszky, A., Herbert-Read, J., Bloch, N.I., Romenskyy, M., Buechel, S.D., Eslava, A.F., Alós, L.S., Zeng, H., Le Foll, A., et al. (2020). Rapid evolution of coordinated and collective movement in response to artificial selection. *Sci. Adv.* 6, eaba3148. <https://doi.org/10.1126/sciadv.aba3148>.

70. Stednitz, S.J., and Washbourne, P. (2020). Rapid Progressive Social Development of Zebrafish. *Zebrafish* 17, 11–17. <https://doi.org/10.1089/zeb.2019.1815>.

71. Stahl, B.A., Peuß, R., McDole, B., Kenzior, A., Jaggard, J.B., Gaudenz, K., Krishnan, J., McGaugh, S.E., Duboué, E.R., Keene, A.C., and Rohner, N. (2019). Stable transgenesis in *Astyanax mexicanus* using the Tol2 transposase system. *Dev. Dyn.* 248, 679–687. <https://doi.org/10.1002/dvdy.32>.

72. Jaggard, J.B., Lloyd, E., Yuiska, A., Patch, A., Fly, Y., Kowalko, J.E., Appelbaum, L., Duboué, E.R., and Keene, A.C. (2020). Cavefish brain atlases reveal functional and anatomical convergence across independently evolved populations. *Sci. Adv.* 6, eaba3126. <https://doi.org/10.1126/sciadv.aba3126>.

73. Kozol, R.A., Conith, A.J., Yuiska, A., Cree-Newman, A., Tolentino, B., Banesh, K., Paz, A., Lloyd, E., Kowalko, J.E., Keene, A.C., et al. (2022). A Brain-wide Analysis Maps Structural Evolution to Distinct Anatomical Modules, 2022. <https://doi.org/10.1101/2022.03.17.484801>.

74. Loomis, C., Peuß, R., Jaggard, J.B., Wang, Y., McKinney, S.A., Raftopoulos, S.C., Raftopoulos, A., Whu, D., Green, M., McGaugh, S.E., et al. (2019). An Adult Brain Atlas Reveals Broad Neuroanatomical Changes in Independently Evolved Populations of Mexican Cavefish. *Front. Neuroanat.* 13, 88. <https://doi.org/10.3389/fnana.2019.00088>.

75. Jaggard, J.B., Stahl, B.A., Lloyd, E., Prober, D.A., Duboué, E.R., and Keene, A.C. (2018). Hypocretin underlies the evolution of sleep loss in the Mexican cavefish. *Elife* 7, e32637. <https://doi.org/10.7554/elife.32637>.

76. Chin, J.S.R., Loomis, C.L., Albert, L.T., Medina-Trenche, S., Kowalko, J., Keene, A.C., and Duboué, E.R. (2020). Analysis of stress responses in *Astyanax* larvae reveals heterogeneity among different populations. *J. Exp. Zool. B Mol. Dev. Evol.* 334, 486–496. <https://doi.org/10.1002/jez.b.22987>.

77. Jeffery, W., Strickler, A., Guiney, S., Heyser, D., and Tomarev, S. (2000). Prox 1 in eye degeneration and sensory organ compensation during development and evolution of the cavefish *Astyanax*. *Dev. Genes Evol.* 210, 223–230. <https://doi.org/10.1007/s004270050308>.

78. Sifuentes-Romero, I., Aviles, A.M., Carter, J.L., Chan-Pong, A., Clarke, A., Crotty, P., Engstrom, D., Meka, P., Perez, A., Perez, R., et al. (2023). Trait Loss in Evolution: What Cavefish Have Taught Us About Mechanisms Underlying Eye Regression. *Integr. Comp. Biol.* iacad032. <https://doi.org/10.1093/icb/iacad032>.

79. Strickler, A.G., Famuditimi, K., and Jeffery, W.R. (2002). Retinal homeobox genes and the role of cell proliferation in cavefish eye degeneration. *Int. J. Dev. Biol.* 46, 285–294.

80. Strickler, A.G., Yamamoto, Y., and Jeffery, W.R. (2007). The lens controls cell survival in the retina: Evidence from the blind cavefish *Astyanax*. *Dev. Biol.* 311, 512–523. <https://doi.org/10.1016/j.ydbio.2007.08.050>.

81. Yamamoto, Y., Stock, D.W., and Jeffery, W.R. (2004). Hedgehog signalling controls eye degeneration in blind cavefish. *Nature* 431, 844–847. <https://doi.org/10.1038/nature02864>.

82. Borowsky, R. (2008). Restoring sight in blind cavefish. *Curr. Biol.* 18, R23–R24. <https://doi.org/10.1016/j.cub.2007.11.023>.

83. Emam, A., Yoffe, M., Cardona, H., and Soares, D. (2020). Retinal morphology in *Astyanax mexicanus* during eye degeneration. *J. Comp. Neurol.* 528, 1523–1534. <https://doi.org/10.1002/cne.24835>.

84. Barriga, E.H., and Mayor, R. (2015). Embryonic cell-cell adhesion: a key player in collective neural crest migration. *Curr. Top. Dev. Biol.* 112, 301–323. <https://doi.org/10.1016/bs.ctdb.2014.11.023>.

85. Bhattacharjee, T., Amchin, D.B., Alert, R., Ott, J.A., and Datta, S.S. (2022). Chemotactic smoothing of collective migration. *Elife* 11, e71226. <https://doi.org/10.7554/elife.71226>.

86. Czirók, A., and Vicsek, T. (2000). Collective behavior of interacting self-propelled particles. *Phys. Stat. Mech. Its Appl.* 281, 17–29. [https://doi.org/10.1016/S0378-4371\(00\)00013-3](https://doi.org/10.1016/S0378-4371(00)00013-3).

87. Eglinton, J., Smith, M.I., and Swift, M.R. (2022). Collective behavior of composite active particles. *Phys. Rev. E* 105, 044609. <https://doi.org/10.1103/PhysRevE.105.044609>.

88. Theveneau, E., and Mayor, R. (2013). Collective cell migration of epithelial and mesenchymal cells. *Cell. Mol. Life Sci.* 70, 3481–3492. <https://doi.org/10.1007/s00018-012-1251-7>.

89. Berlinger, F., Gauci, M., and Nagpal, R. (2021). Implicit coordination for 3D underwater collective behaviors in a fish-inspired robot swarm. *Sci. Robot.* 6, eabd8668. <https://doi.org/10.1126/scirobotics.abd8668>.

90. Werfel, J., Petersen, K., and Nagpal, R. (2014). Designing collective behavior in a termite-inspired robot construction team. *Science* 343, 754–758. <https://doi.org/10.1126/science.1245842>.

STAR★METHODS

KEY RESOURCES TABLE

REAGENT or RESOURCE	SOURCE	IDENTIFIER
Software and algorithms		
Python version 3.10	Python Software Foundation	https://www.python.org
Trilab-tracker version 0.1.2	Patch et al. ⁵³	https://github.com/yffily/trilab-tracker/tree/0.1.2
Analysis script and tracks	This manuscript	https://doi.org/10.17632/z8d7zf3xf
Miniconda	Anaconda, Inc.	https://docs.conda.io/en/latest/miniconda.html

RESOURCE AVAILABILITY

Lead contact

Further information and requests for resources and reagents should be directed to and will be fulfilled by the lead contact, Johanna Kowalko, (jok421@lehigh.edu).

Materials availability

This study did not generate new unique reagents.

Data and code availability

- All tracking data has been deposited at Mendeley data and is publicly available as of the date of publication. See [key resources table](#).
- Original code has been deposited at Mendeley data and is publicly available as of the date of publication. The latest version of tracking software is available at Github. See [key resources table](#).
- Any additional information required to reanalyze the data reported in this paper is available from the [lead contact](#) upon request.

EXPERIMENTAL MODEL AND SUBJECT DETAILS

Animal care

Surface and cave embryos were collected the morning after spawning and placed in glass Pyrex bowls filled with conditioned fish water. >1 dpf embryos were randomly sorted into groups of 50 in 350 ml glass Pyrex bowls. After being assayed at 7 dpf, fish were group-housed in 2L plastic tanks where they remained until 14 dpf. Fish were then transferred in groups into 6L tanks on a filtered aquatic housing system, where they remained for the rest of the experiment. Prior to being placed on the system, routine water changes were performed. Beginning at 6 dpf, fish were fed twice a day on weekdays and once a day on weekends. All individuals received a combination of brine shrimp and GEMMA Micro. All cave fish used in these assays were descendants of adult fish originally collected from the Pachón cave, and all surface fish used were descendants of individuals originally collected from rivers in Mexico and Texas. All protocols were approved by the institutional animal care and use committee (IACUC) of Florida Atlantic University, and all fish were kept in Florida Atlantic University fish facilities. Water temperatures were maintained at $23 \pm 1^\circ\text{C}$ and light:dark cycles were kept at 14:10, with a light intensity between 24 and 40 lux using cool fluorescent bulbs. Assays were performed at 7 dpf, 28 dpf, 42 and 70 dpf. At these stages, sex cannot be determined. Thus, sex was not recorded for individuals in these assays.

METHOD DETAILS

Behavioral experiments

All fish were fed to satiety at least 1 hour before beginning assays. Before being assayed, fish were carefully netted into a holding tank for one minute and then were gently poured into a circular arena and allowed to acclimate for 10 minutes. After the acclimation period, behavior was recorded for a duration of 20 minutes

at 30 fps with a video camera (FLIR; GS3-U3-23S6M-C) equipped with a wide-angle c-mount lens (Edmund Optics; HP Series 12 mm fixed focal length lens) mounted above the center of the arena on a custom stand constructed from polyvinyl chloride (PVC) tubing (Figure S7A). Assays were recorded as series of .RAW files which included timestamps for each frame. Arena diameters were increased across developmental time-points assayed in order to maintain approximately a ratio of 22 body lengths per arena diameter (Table 1; Figures S7B, S8A, and S8B). Arenas were 3D printed (Creality; CR10MAX) in black polylactic acid (PLA) and adhered onto a sheet of clear acrylic with acrylic cement and then rendered waterproof with a layer of silicone along the base of the outer edge of the arena. Arenas were placed on top of custom-made white acrylic boxes (76 x 76x 14 cm) that diffused light emitted by white-light LED strips placed under the box.

QUANTIFICATION AND STATISTICAL ANALYSIS

Tracking

RAW files were compiled into videos (.mkvs) and subsequently processed using version 0.1.2 of the custom python tracking library trilab-tracker⁵³ (located at <https://github.com/yffly/trilab-tracker/tree/0.1.2>), which extracts the positions and orientations of fish. All tracking and orientation data were manually verified, and corrections were applied when necessary. Arena edges were selected manually and used to convert pixels to centimeters based on the arena diameter. For and Figures 3, 4, 5, S3, S4, S10, and S11, trajectories were smoothed using a five-frame Savitzky-Golay filter (scipy.signal.savgol_filter with window_length=5). Trajectories were not smoothed for other figures. Fish velocities and accelerations and their angular counterparts were computed using standard finite difference formulas:

$$\vec{v}_i = \frac{\vec{r}_{i+1} - \vec{r}_i}{dt}, \vec{a}_i = \frac{\vec{r}_{i+1} + \vec{r}_{i-1} - 2\vec{r}_i}{dt^2}, \omega_i = \frac{\varphi_{i+1} - \varphi_i}{dt}, \alpha_i = \frac{\varphi_{i+1} + \varphi_{i-1} - 2\varphi_i}{dt^2} \quad (\text{Equation 1})$$

where \vec{r}_i is the fish's position vector in frame number i , \vec{v}_i is its velocity vector, \vec{a}_i is its acceleration vector, $\vec{\alpha}_i$ is the angle between the x axis and the fish's orientation, ω_i is the fish's angular velocity, and α_i is the fish's angular acceleration.

Mock group formation

Nearest neighbor alignment, nearest neighbor distance, and interindividual distance of real fish groups were compared to mock groups generated by extracting the positions of individuals that were not assayed together and combining them to form groups of five fish. The process of generating mock groups began by making a list of all assays for a given age and population. We then found all possible combinations of five of these assays and randomly chose a single fish from each of the assays. The tracks of these fish were then grouped to form a mock group. The number of mock groups generated this way is,

$$C(n, r) = \frac{n!}{(n - r)!r!}, \quad (\text{Equation 2})$$

where n is the number of real trials with the right age and population and $r = 5$ is the number of fish per trial. Since the identity of the fish picked from each assay is drawn randomly, repeating the mock group formation process yields a different outcome each time. In order to assess the associated variability, the outcomes of 10 iterations of the mock group formation process were compared via Kruskal-Wallis and found to be similar. The results of the first run were used for all comparisons between mock groups and real groups.

Orientation and distance analyses

Pair distance was calculated by finding the distance between the center points of two fish. Interindividual distance was calculated by finding the pair distance between a focal fish and all other fish in the trial and nearest neighbor distance was calculated by finding the minimum pair distance for each fish in each frame. Pair angle was calculated by finding the difference between the orientations of two fish. Nearest neighbor pair angle was calculated by finding the pair angle between the focal fish and its nearest neighbor. Nearest neighbor pair orientations, nearest neighbor distances, and interindividual distances were measured for real and mock data. Before hypothesis testing, distributions of distance and pair angle data were assessed using Shapiro-Wilk tests for real data and Kolmogorov-Smirnov tests for mock data to account for differences in quantities of real and mock groups. Comparisons were made between real and mock data of the same age and population using a student's t-test if both the real and mock data were found to be normally distributed or a Mann-Whitney U test if either dataset was found to be non-normal. Throughout the

text, means are reported for data that were found to be normally distributed and medians are reported for data that were not found to be normally distributed. As fish can develop at different rates, we also assessed the relationship between these metrics and body length. While analyses herein were conducted according to the age of the fish, body length is also a good predictor of changes in proximity in surface fish (Figure S9).

The correlations between swimming speed and proximity and alignment were assessed by calculating the Spearman's rank correlation coefficient for each age and population using the mean trial swimming speed and mean nearest neighbor distance, mean interindividual distance, or mean nearest neighbor pair angle for each frame of each trial.

Density heatmaps

Density heatmaps (Figure 3) show the density of fish around a focal fish located at the center of the heatmap, facing up. First a focal fish is picked. The focal fish's coordinate system is defined, whose origin is the center point of the focal fish and whose y axis points in the direction faced by the focal fish. The coordinates of every other fish in the trial are computed in this coordinate system, normalized by the tank radius, then binned according to Figure 3. The radius bin edges are 0, 0.05, 0.1, 0.15, 0.2, 0.3, 0.4, and 0.5. The value of each bin is the probability of finding a fish in that bin, divided by the area of that bin. The result is in fish per square tank radii.

Force heatmaps

Force heatmaps (Figures 4 and 5) show the average speeding and turning forces of the focal fish when another fish is present nearby as a function of the location of that other fish. The speeding force is the component of the focal fish's acceleration that is parallel to its own orientation, i.e., the focal fish's tangential acceleration. The turning force is the component of the focal fish's acceleration that is perpendicular to its own orientation, i.e., the focal fish's normal acceleration. The latter is counted positively if it points to the right of the fish and negatively to the left. The acceleration is computed using finite differences. The orientation is obtained from the fish's body shape. Both accelerations are normalized by the average swimming speed. The average is computed over every fish from the same population and age cohort. Once a focal fish has been picked, the coordinates of the other fish in the trial are computed and binned as for density maps. The value of a bin is the average of the focal fish's speeding or turning force over every frame in which there was a second fish in that bin. Overall, our method is similar to previous analysis,¹¹ except our bins are based on polar rather than cartesian coordinates and they do not overlap.

Attractive speeding and turning force

The speeding force is positive when the focal fish speeds up and negative when it slows down. If the focal fish uses speed changes to get closer to its neighbors, we expect it to speed up when the neighbor is ahead but slow down when the neighbor is behind. Conversely, speeding up when the neighbor is behind and slowing down when the neighbor is ahead suggests repulsion. Therefore, we define the attractive speeding force to be equal to the speeding force when the neighbor is ahead but minus the speeding force when the neighbor is behind. With this definition, positive values indicate attraction and negative values indicate repulsion. Similarly, we define the attractive turning force to be equal to the turning force when the neighbor is on the right side of the focal fish but minus the turning force when the neighbor is on the left side of the focal fish. With this definition, positive values indicate attraction (the focal fish's trajectory is curving towards the neighbor) and negative values indicate repulsion (the focal fish's trajectory is curving away from the neighbor). The attractive speeding and turning forces are then averaged over all possible locations of the neighbor fish, restricted to the range of distances where we expect attraction. The density heatmap for 70 dpf surface fish, which exhibit robust attraction, shows a ring of increased probability between about 0.05 and 0.4 tank radii around the focal fish, with a peak around 0.15 tank radii. Therefore, we expect interactions to be repulsive on average between 0.05 and 0.15 tank radii and attractive on average between 0.15 and 0.4 tank radii. Short range repulsion may be simple collision avoidance, so we focus on the attractive range, i.e., distances between 0.15 and 0.4 tank radii. The average over neighbor positions is weighted by each bin's area, i.e., all possible location of the neighbor fish within the allowed distance range are treated equally, independently of the likeliness of finding a fish there. Weighing instead by the likeliness of finding a fish in each bin yields similar results. Speeding and turning force violin plots are the difference between real (Figure S10) and mock data (Figure S4).

Aligning angular acceleration

Just like the attractive speeding and turning forces are defined to be positive when they contribute to decreasing the distance to the focal fish's neighbor, the aligning angular acceleration is defined to be positive when it contributes to decreasing the angle between the headings of the focal fish and its neighbor. We start with the angular acceleration, which is positive when the focal fish attempts to rotate counterclockwise and negative when it attempts to rotate clockwise, then flip the sign if the angle between the heading of the focal fish and the heading of the neighbor fish is negative (between -180° and 0°). We then average over neighbor locations whose distance to the focal fish is between 0.05 and 0.4 tank radii. The upper bound (0.4 tank radii) is the same use to compute the average attractive speeding and turning forces. The lower bound (0.05 tank radii) is lower than the one used for the average attractive speeding and turning forces (0.15 tank radii) because while we expect schooling fish less than 0.15 tank radii away from each other to attempt to maintain alignment while they adjust their distance to each other. Angular acceleration violin plots are the difference between real and mock data (Figures S10E and S10F).

Density, force, and angular acceleration mock data

The mock data used in Figures 4, 5, S10E, and S10F were obtained by averaging the relevant quantity (speeding force, turning force, or angular acceleration) over every possible pair of fish taken from two different trials. This is equivalent to averaging over every pair of fish from the same mock trial and every possible mock trial (every possible group of 5 fish taken from 5 different real trials). This only works because all quantities shown Figures 4, 5, S10E, and S10F are pairwise. It would not work for, e.g., a quantity involving the nearest neighbor as the identity of the nearest neighbor depends on the position of every fish in the trial.

Statistical analysis of attractive forces and aligning angular acceleration

After subtracting the mean mock value, the distribution of attractive speeding force, attractive turning force, or aligning angular acceleration was tested for normality using a Shapiro-Wilk test. Data assessed as non-normally distributed via the Shapiro-Wilk test were analyzed using a Wilcoxon Signed-Rank Test. The distributions of the remaining data were assessed via visual inspection of Q-Q plots (Figure S11), and data which showed departures from normality were also analyzed using a Wilcoxon Signed-Rank Test. Normally distributed data were analyzed using a one-way t-test. Because positive values for these measurements indicate behaviors that increase either proximity or alignment, and negative values indicate behaviors that either increase distance between individuals or decrease alignment, comparisons to zero allow for the identification of how speeding and turning contribute to proximity and alignment in these analyses. Complete results of the statistical tests mentioned here can be found in Figures S5 and S6, and Q-Q plots illustrating the distributions of these data can be found in Figure S11.

Analysis software

Figures were generated and analyses performed using custom Python 3 scripts available at <https://doi.org/10.17632/z8d7zf3xf>. The Pandas and Numpy libraries were used for data organization and analysis. Statistical analysis was performed using the following python libraries: scipy.stats for Kolmogorov-Smirnov, Shapiro-Wilk, Kruskal-Wallis, Mann-Whitney U, Wilcoxon Signed-Rank test, and t-tests; and scikit_posthocs for Dunn's test. Figures were generated using the Matplotlib and Seaborn libraries.